Cyclic citrulinated MBP$_{87-99}$ peptide stimulates T cell responses: implications in triggering disease

Vasso Apostolopoulos[a],*, George Deraos[b], Minos-Timotheos Matsoukas[c], Stephanie Day[d], Lily Stojanovska[a], Theodore Tselios[b], Maria-Eleni Androutsou[b,e], John Matsoukas[b,e],

[a] *Centre for Chronic Disease, College of Health and Biomedicine, Victoria University, VIC 3021 Australia*
[b] *Department of Chemistry, University of Patras 26500 Greece*
[c] *Department of Pharmacy, University of Patras 26500 Greece*
[d] *Immunology and Vaccine Laboratory, Austin Research Institute, Melbourne VIC Australia*
[e] *ELDrug, Patras Science Park, Patras, Greece*

*Corresponding author.
E-mail address: vasso.apostolopoulos@vu.edu.au

Running Title: Citrulinated MBP$_{87-99}$ Peptides

Abbreviations: MS, multiple sclerosis; Th, T helper; MBP, myelin basic protein; APL, altered peptide ligand; TCR, T cell receptor; MHC, major histocompatibility complex; HLA, human leukocyte antigen; PAD, peptidylarginine deiminase; Cit, citrulline; TLC, thin layer chromatography; MD, molecular dynamics;

ABSTRACT

Amino acid mutations to agonist peptide epitopes of myelin proteins have been used to modulate immune responses and experimental autoimmune encephalomyelitis (EAE, animal model of multiple sclerosis). Such amino acid alteration are termed, altered peptide ligands (APL). We have shown that the agonist myelin basic protein (MBP) 87-99 epitope (MBP$_{87-99}$) with crucial T cell receptor (TCR) substitutions at positions 91 and 96 (K^{91},P^{96} (TCR contact residues) to R^{91},A^{96}; [R^{91},A^{96}]MBP$_{87-99}$) results in altered T cell responses and inhibits EAE symptoms. In this study, the role of citrulination of arginines in [R^{91},A^{96}]MBP$_{87-99}$ peptide analog was determined using *in vivo* experiments in combination with computational studies. The immunogenicity of linear [Cit^{91},A^{96},Cit^{97}]MBP$_{87-99}$ and its cyclic analog - cyclo(87-99)[Cit^{91},A^{96},Cit^{97}]MBP$_{87-99}$ when conjugated to the carrier mannan (polysaccharide) were studied in SJL/J mice. It was found that mannocylated cyclo(87-99)[Cit^{91},A^{96},Cit^{97}]MBP$_{87-99}$ peptide induced strong T cell proliferative responses and IFN-gamma cytokine secretion compared with the linear one. Moreover, the interaction of linear and cyclic peptide analogs with the major histocompatibility complex (MHC II, H2-IA^{s}) and TCR was analyzed using molecular dynamics simulations at the receptor level, in order to gain a better understanding of the molecular recognition mechanisms that underly the different immunological profiles of citrulinated peptides compared to its agonist native counterpart MBP$_{87-99}$ epitope. The results demonstrate that the citrulination of arginine in combination with the backbone conformation of mutated linear and cyclic analogs are significant elements for the immune response triggering the induction of pro-inflammatory cytokines.

1. Introduction

Multiple sclerosis (MS) is associated with dysregulation of the immune system, where auto antigens stimulate antibody and CD4^{+} Th1 cell responses to self antigens, such as, myelin basic protein (MBP), proteolytic protein and myelin oligodendrocyte glycoprotein.[1, 2] This results in pro-inflammatory cytokines (IFN-gamma (γ), TNF-alpha) and demyelination of the myelin sheath. More recently, Th17 cells, secreting IL-17A and IL-17F, have been associated with increased risk of MS.[3]
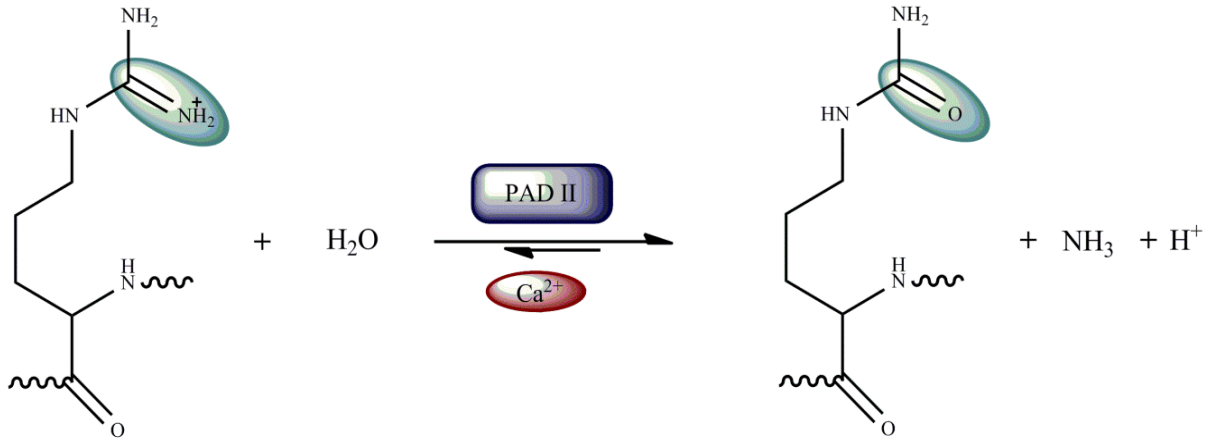
Mutated peptides, altered peptide ligands (APL), are defined as amino acid mutations at T cell receptor (TCR) contact residues of the wild type peptide, which alters immune responses, to antagonists, agonists or superagonists.[4, 5] Methods into altering immune responses in MS, have involved APLs derived from the self autoimmune agonist (wild type) peptide from MBP, residues within 83-99, with the aim to shift pro-inflammatory T helper (Th)1 (IFN-γ) responses to the anti-inflammatory Th2 (IL-4, IL-10) responses.[6-10] In fact, we have preciously shown, by x-ray crystallography of the MHC-peptide-TCR complex, that modulation of the immune response to a peptide (i.e. changing activity from TCR agonistic to antagonistic or superagonistic) was determined by slight changes in the interaction between the complementarity-determining three loops of the TCR and the altered side chains of the peptide epitope.[4] APL in complex with MHC and/or TCR, from vesicular stomatitis virus and human immunodeficiency virus, only minor conformational changes in the peptide side chains were sufficient enough to lead to profound biological alterations.[11, 12] Likewise, Likewise, APLs derived from the gp100$_{44-59}$ epitope, associated with melanoma, when bound to HLA-DR4, altered the immune response. This was due to the very subtle, yet crucial changes due to the difference in the mode of epitope side-chain interactions with the TCR.[13] In MS, APLs of the human immunodominant MBP$_{83-99}$ or the shorter MBP$_{87-99}$ epitopes have been shown to alter immune responses by diverting Th1 (IFN-γ) to Th2 (IL-10) profile. APLs derived from MBP$_{83-99}$ epitope were used in phase I human clinical trials with varying responses and side effects.[14-17] In addition, we previously demonstrated that linear APL of the wild type MBP$_{87-99}$ with mutations at K^{91}, P^{96} (TCR contact residues) to R^{91}, A^{96}; [R^{91}, A^{96}]MBP$_{87-99}$ protected animals from experimental autoimmune encephalomyelitis (EAE) and it was not able to stimulate the encephalitogenic T cells as it did not interact strongly with TCR.[18-23] Cyclization of [R^{91}, A^{96}]MBP$_{87-99}$ peptide[7] completely blocked the development of EAE in rats.[22, 24] Using, peripheral blood mononuclear cells from MS patients cultured with linear or cyclic [R^{91}, A^{96}]MBP$_{87-99}$ peptides altered cytokine profile of dominant Th1 cytokines to increased Th2/Th1 cytokine ratio.[25]

Protein citrullination is a post-translational modification of peptidyl-arginine, which plays a role in normal functioning of the immune system.[26] However, it has been suspected that citrullination plays a pathophysiological role in a number of conditions, including, psoriasis, chronic obstructive pulmonary disease, multiple sclerosis, inflammatory bowel

disease, cancer, rheumatoid arthritis and in degenerative diseases including dementia and Alzheimer's disease.[27] During the citrulination process, the positively charged amino acid Arginine (Arg) is converted into the neutral amino acid Citrulline (Cit) (Scheme 1), which is regulated by peptidylarginine deiminases (PAD). As a result, a non-compact structure is created, leading to degradation by cathepsin D. The post-translational modification of MBP, results in protein unfolding, degradation catalyzed by proteolytic enzymes and subsequently releasing new citrulinated peptide epitopes that could be immunogenic, hence, triggering disease (Schemes 1, 2).[28-30] In fact, citrulinated proteins of MBP are present in white matter lesions in the central nervous system in MS.[31] In addition, serum (antibodies) from patients with MS react to a citrulinated isomer of MBP (MBP-C8)[32], as well as being recognized by CD4$^+$ T cells from MS patients.[33]

SJL/J mice (H-2^s haplotype; H2-IA^s) is used to induce experimental autoimmune encephalomyelitis (an MS model in mice), as several histopathological, clinical and immunological outcomes mimic those of human MS.[34] In SJL/J mice, residues from the encephalitogenic epitope MBP$_{83-99}$ bind with high affinity to H2-IA^s with the minimum epitope being MBP$_{87-99}$.[35] Based on the minimum binding peptide MBP$_{87-99}$, we designed and synthesized citrulinated analogs in order to determine their immunogenic potential. We previously demonstrated that two citrullinated peptides, linear [Cit^{91},A^{96},Cit^{97}]MBP$_{87-99}$ (linear-Cit) and cyclo(87-99)[Cit^{91},A^{96},Cit^{97}]MBP$_{87-99}$ (cyclic-Cit) that resulted from citrullination of antagonists, linear [R^{91},A^{96}]MBP$_{87-99}$ and cyclo(87-99)[R^{91},A^{96}]MBP$_{87-99}$ peptides were able to stimulate inflammatory Th1 polarization of peripheral blood mononuclear cells from MS patients.[28] Herein, we studied the Immunogenicity of the two citrullinated peptides, linear-Cit and cyclic-Cit conjugated to KLH and reduced mannan, in SJL/J mice. We demonstrate that cyclic-Cit-KLH-reduced mannan induced strong T cell proliferative responses and IFN-γ cytokine secretion. In addition, by molecular modeling, linear-Cit and cyclic-Cit were compared to linear native MBP$_{87-99}$ agonist peptide (linear-native), in order to gain insights in the molecular interactions with H2-IA^s and hence the T cell receptor. These results give further evidence that citrulinated MBP peptides may potentially trigger disease in susceptible individuals.[36]
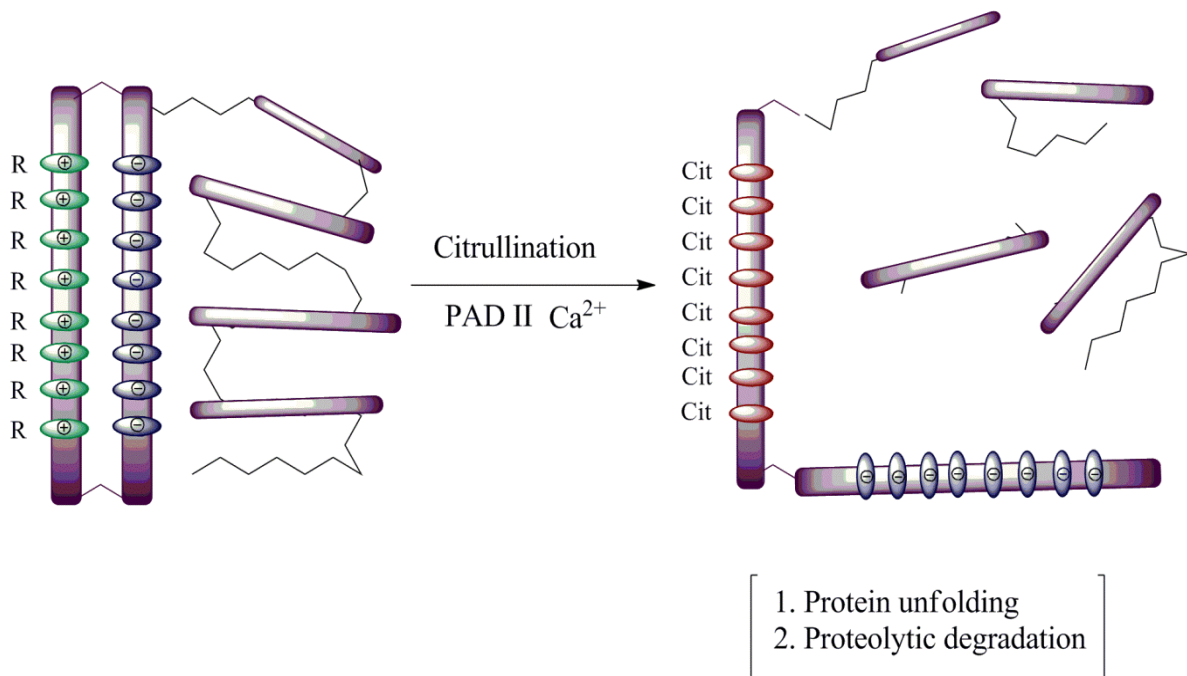
Scheme 1. Post-translational modification of Arginine into Citrulline catalyzed by PAD.


Scheme 2. Unfolding and proteolytic degradation of MBP protein as a result of citrulination.

2. Results and discussion

Citrullination is an enzymatic conversion of arginine to citrulline on proteins via PAD enzymes. The pathogenisis of MS is still not clear, however, high levels of PAD is present in the white matter of brain suggesting a biochemical pathway in the pathogenisis of MS.[37] Several charged isomers of MBP exist with C1 (most common, most cationic) and C2, C3, C4, C5, C6, C7 and C8 the least cationic are a result of citrullination, deamindation or methylation. In MS patients an increase in MBP citrullination is noted in brain tissue as well as enhanced T cell responsiveness to MBP-C8.[38] Furthermore, in rats, MBP-C8 is immunogenic resulting in T cells that induce experimental autoimmune encephalomyelitis. To further understand the role of citrullination in triggering T cells and cytokines in MS, we determined the immunogenic potential of citrullinated MBP_{87-99} peptides. Hence, linear-native, linear-Cit and cyclic-Cit peptides were synthesized in-house (Department of Chemistry, University of Patras, Greece) and were > 98 % pure as analyzed by HPLC and Electron Spray Ionization Mass Spectrometry (ESI-MS).

2.1. Cyclic-Cit peptide-KLH-reduced mannan, induce strong T cell proliferative responses

SJL/J mice were immunized with linear-Cit and cyclic-Cit peptides, conjugated to keyhole limpet hemocyanin (KLH) and reduced mannan. KLH acts as a linker between peptide and reduced mannan. We have studied in detail the ability of mannan as a carrier to generate immune responses in various model systems. Mannan binds to C-type lectins, including the mannose receptor on antigen presenting cells,[39,40] and generates immune responses to peptides. Spleen cells were isolated and assessed for T cell stimulation using the T cell proliferation assay. Mice immunized with cyclic-Cit peptide-KLH-reduced mannan, induced strong T cell proliferative responses when restimulated *in vitro* with cyclic-Cit peptide (red) or linear-Cit (green). Interestingly linear-native peptide did not stimulate T cell responses (blue) which were similar to background non-stimulated T cells (black). Mice immunized with linear-Cit peptide-KLH-reduced mannan, and, naïve mice, did not induce T cell responses (Fig. 1). As the T cell epitopes used are CD4$^+$ epitopes it is likely that CD4$^+$ T cells are proliferating. Hence, cyclic-Cit peptide-KLH-reduced mannan induce srong T cell proliferative responses (Table 1).

Absorbance at 490 nm

Days after peptide recall stimulation
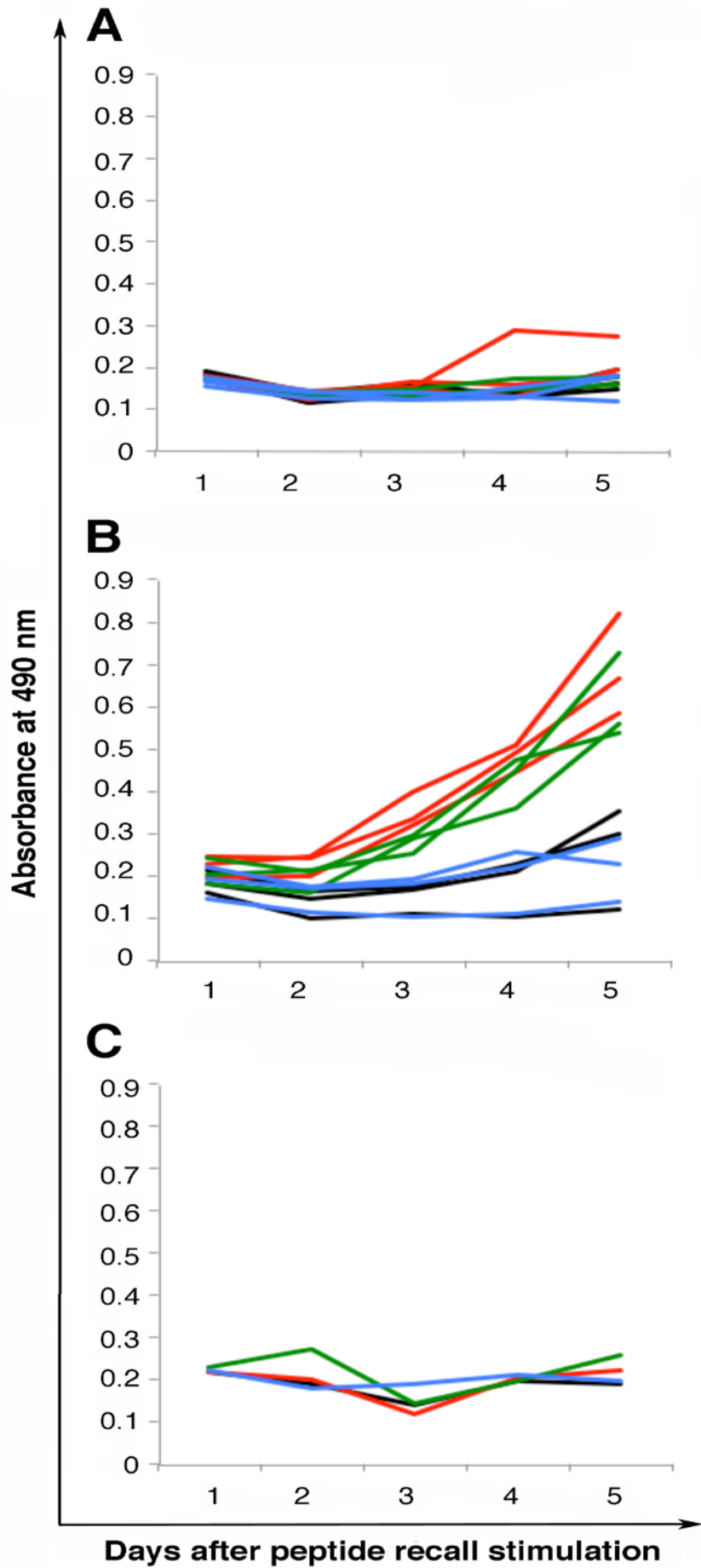
Figure 1. T cell Proliferation assay from mice immunized with (A) linear-Cit peptide-KLH-reduced mannan, (B) cyclic-Cit peptide-KLH-reduced mannan, or, (C) no immunization (naïve mice). Spleen cells were restimulated with either, cyclic-Cit peptide (red), or linear-Cit peptide (green), linear-native (blue), or, no recall peptide (black). Figure shows three mice/group where each line depicts each individual mouse. Individual mouse curves are shown to demonstrate variability between each immunized mouse. All experiments were repeated three times and representative data are shown.

2.2. Cyclic-Cit peptide-KLH-reduced mannan induce strong IFN-γ and IL-4 cytokine responses

The native peptide, MBP$_{87-99}$, is pathogenic in mice and humans, leading to the induction of Th1 pro-inflammatory cytokines. Mutating 2 TCR contact residues at positions 91, 96, [R^{91},A^{96}]MBP$_{87-99}$ (altered peptide ligand, APL), changes the immunogenic profile from Th1 to Th2 with high levels of IL-4 and lower IFN-γ[41] ; citrulination of this linear and cyclic APL stimulates inflammatory Th1 polarization of peripheral blood mononuclear cells from MS patients.[28] Herein, we assessed the immunogenic potential of linear and cyclic-Cit peptides in SJL/J mice. Spleen cells were isolated and assessed for T cell cytokine production (IFN-γ, IL-4, IL-10) using ELISpot assay. Mice immunized with cyclic-Cit peptide-KLH-reduced mannan induced strong IFN-γ and IL-4 cytokine production by T cells after recall with cyclic-Cit peptide (red) or linear-Cit peptide (green), and to a lesser extent after recall with linear-native peptide (blue) (Fig. 2A, B); no IL-10 cytokine secretion was noted (Fig. 2C). Conversely, mice immunized with linear-Cit peptide-KLH-reduced mannan induced low levels of IL-4 (Fig. 2B) but no IFN-γ or IL-10 after all recall peptides; responses were similar to non-immunized naïve mice (Fig. 2A, C, Table 1). This data demonstrates that dominant pro-inflammatory (Th1) cytokine responses are generated following immunization with cyclic-Cit peptide. In MS, pro-inflammatory cytokine responses are one of the contributing factors to disease progression and demyelination. Thus, as cyclic-Cit peptide induces a strong IFN-γ response it is likely that citrulination may be involved in triggering of disease. To understand the mechanism of citrulinated peptides in disease, further detailed analysis of other cytokines, such as IL-1, IL-8, IL-13, IL-17 need to be measured as well as experimental autoimmune encephalomyelitis experiments following linear or cyclic-Cit peptide immunization need to be conducted.
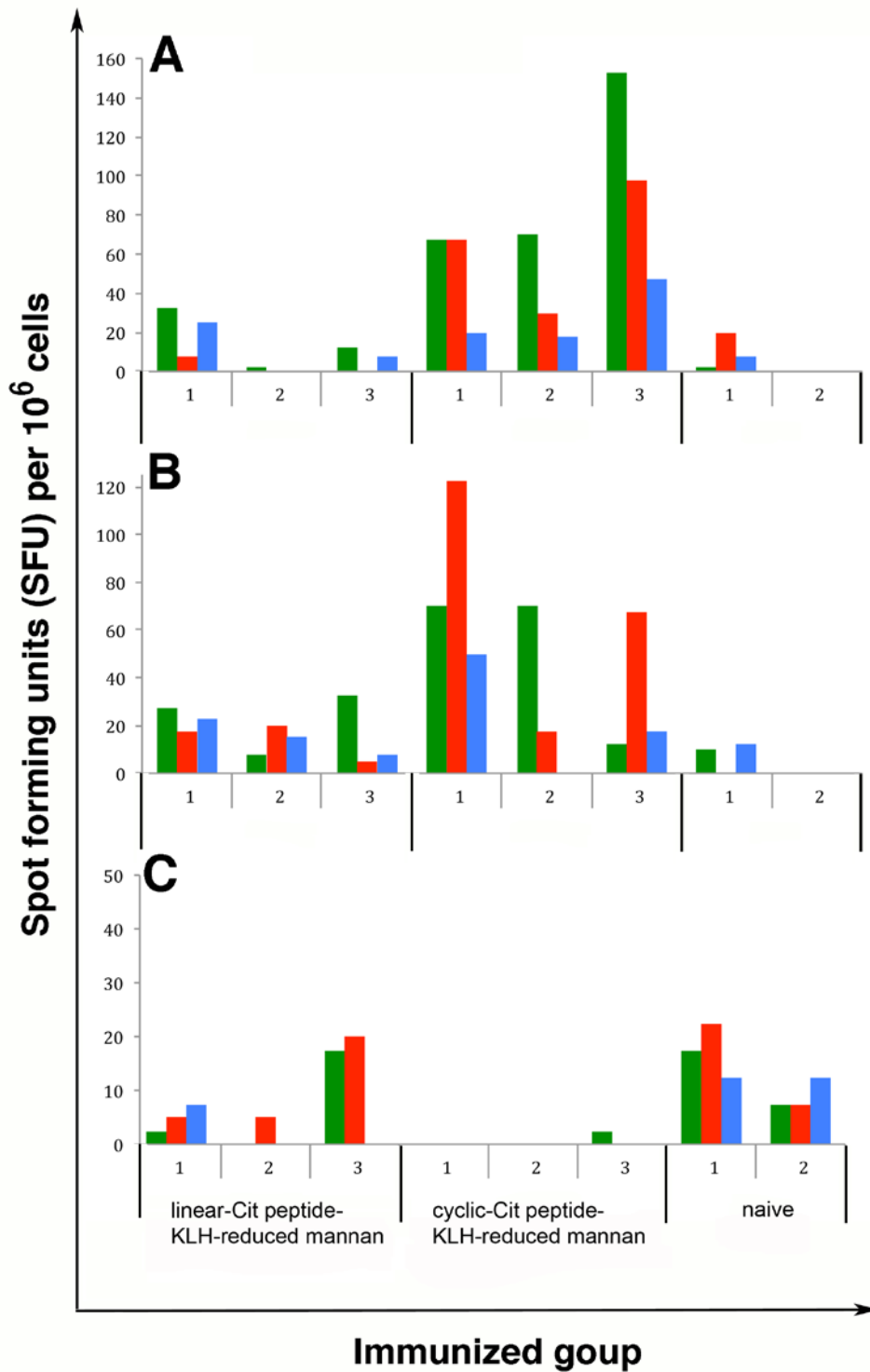
Figure 2. Cytokine induction (A) IFN-γ, (B) IL-4, (C) IL-10, from mice immunized with linear-Cit peptide-KLH-reduced mannan, cyclic-Cit peptide-KLH-reduced mannan, or, non immunized (naïve mice). Spleen cells were restimulated with either, cyclic-Cit peptide (red), linear-Cit peptide (green) or linear-native peptide (blue). Figure shows a representative of three mice/group where three individual mouse responses are shown to show variability between each mouse. Experiments were repeated 3 times.

Table 1. Summary of immune responses induced by peptide immunization

Peptide conjugate	Immune response			
	T cell proliferation	IL-4	IL-10	IFN-γ
Linear-Cit KLH-reduced mannan	-	+/-	-	-
Cyclic-Cit KLH-reduced mannan	+	+	-	+
Naïve control mice	-	-	-	-

2.3. Interactions of linear-Cit, cyclic-Cit and linear-native in complex with MHC class II, H2-IA^s

Several MBP peptides with the minimal containing 87-99 sequence (MBP$_{87-99}$ peptide) have been co-crystallized in MHC clefts. We traced these crystal structures, to study the binding orientation of these peptides (Table 2). They were found to bind in 2 different ways. In HLA-DR2b and HLA-DQ1, pockets P1, P4, P6, P9 are occupied by V^{87}, F^{90}, N^{92} and T^{95} respectively (PDB IDs: 1ymm,[42] 1bx2[43] and 3pl6[44]) as shown in Table 3, this binding mode will be referred to as binding pattern B. In the pattern A, present in HLA-DR2a, the peptide register is shifted by three residues, compared to the HLA-DR2b crystal structures and in which the pockets are occupied by the side chains of F^{90}, I^{93}, T^{95} and T^{98} (PDB IDs: 1fv1,[45] 1hqr[46] and 1zgl[47]). Binding pattern A occurs, because of the presence of G86B and K71B in DR2a, compared to V86B and A71B in DR2b. The result is a wider P1 and a shallower P4 pocket in DR2a.[45] In the case of binding pattern B, P4 is much wider, therefore the extended bulky aromatic F^{90} side chain has plenty of space and enters P4, resulting in this binding mode. H2-IA^s has a similarly structured pocket to DR2b, with the main differences to HLA-DR2b being G66A, F11B, G13B, T71B and E74B instead of D66A, P11B, R13B, A71B and A74B (Fig. 3A). In specific, the presence of T71B and V86B results in a wide P4 and shallow P1 respectively. Thus, binding pattern B was considered as the predominant one and therefore docking of the linear-native and linear-Cit peptides within the MHC cleft of H2-IA^s homology model, was performed accordingly.

In order to generate the molecular dynamics simulations starting models, the MBP$_{87-99}$ peptide was docked in the H2-IA^s MHC cleft using the peptide binding pattern B from the HLA-DR2b (PDB ID: 1bx2[43]) crystal structure. Citrulline and alanine residues for [Cit^{91},A^{96},Cit^{97}]MBP$_{87-99}$, were manually mutated in the binding site. In order to explore the different possibilities of the cyclic peptide's docking orientation, it was docked in four different poses, with the coordinates of F^{90} and N^{92} in pockets P4 and P6 being maintained. All the complexes were energy minimized prior to the MD simulations.

Table 2. List of crystal structures with MBP peptides a containing the minimal 89-96 sequence binding to MHC molecules. The two different binding patterns refer to the positioning of the peptides in the cleft.

_____

Haplotype	MBP epitope*	PDB ID	Resolution (Å)	Reference	Binding pattern
HLA-DR2b	83-96	1BX2	2.6	[43]	B
HLA-DR2a	84-103	1FV1	1.9	[45]	A
HLA-DR2a	89-98	1HQR	3.2	[46]	A
HLA-DR2b	83-96	1YMM	3.5	[42]	B
HLA-DR2a	87-100	1ZGL	2.8	[47]	A
HLA-DQ1	84-97	3PL6	2.55	[44]	B

*Numbering of MBP epitope residues refers to the numbering used in this study (V^{87}-H^{88}-F^{89}-F^{90}-K^{91}-N^{92}-I^{93}-V^{94}-T^{95}-P^{96}-R^{97}-T^{98}-P^{99})

Table 3. Occupation of the standard MHC defined pockets by residues present in the MBP analogs in the two different binding patterns observed in already crystallized complexes.

_____

Binding Pattern	P1	P2	P3	P4	P5	P6	P7	P8	P9
A	F^{90}	K^{91}	N^{92}	I^{93}	V^{94}	T^{95}	P^{96}	R^{97}	T^{98}
B	V^{87}	H^{88}	F^{89}	F^{90}	K^{91}	N^{92}	I^{93}	V^{94}	T^{95}

The molecular dynamics simulations showed stable binding for the MBP residues 87-95 occupying pockets P1-P9 for linear-Cit, as well as linear-native , which were both stable during the simulations (Fig. 3B). In both simulations of the linear peptides, residues 96-99 appeared to have fluctuations, despite the high rigidity of the rest of the peptide which is deeper located in the cleft. The cyclic peptides were docked in 4 different orientations to determine the most favorable interacting pose. All initial cyclic peptide conformations had in common the occupancy of F^{90} and N^{92} in pockets P4 and P6 (Fig. 3C), in order to evaluate their stability in the MHC cleft. According to the RMSDs of the cyclic peptide (Fig. 3B), the second simulation (b) was the most stable and could provide a basis for cyclic-Cit peptide recognition by this specific MHC haplotype. Therefore, simulation (b) was used for the analysis regarding cyclic-Cit peptide binding mode. During the simulation, residues F^{90} and N^{92}, occupy in a consistent manner the main anchor positions P4 and P6. As it can be seen in Fig. 4A, distant pockets P1 and P9 are not occupied due to the cyclic nature of the peptide. However, several other interactions, mainly hydrophobic, may assist the recognition of the cyclic-Cit peptide, such as the aromatic-aromatic interaction between H^{88} and H81B, the F^{89} side chain aromatic

ring with G58A and the hydrophobic interaction between I^{93} and Y61B (Fig. 4B). Side chain electrostatic interactions that were observed during the simulation were H^{88} with N82B, Cit^{91} with Q70B and Cit^{91} with E74B (Fig. 4A).

Comparison of the binding modes of linear-Cit and cyclic-Cit peptides derived from the molecular dynamics simulations and the crystal structure of $MBP_{85\text{-}98}$,[48] some speculation can be made on their important structural elements for MHC binding. Superimposition of the representative MD conformations of linear-Cit and cyclic-Cit, compared to linear peptide were found in the $MBP_{85\text{-}98}$ - HLA-DR2b crystal structure (Fig. 4B).[48] $MBP_{85\text{-}98}$ and linear-Cit share many similarities in their positioning in the cleft and the groove anchoring pockets P1, P4, P6 and P9 are similarly occupied by side chain pharmacophore groups of V^{87}, F^{90}, N^{92} and T^{95}. F^{90} has a side chain rotameric change due to the existence of $V^{78}B$ in the $H2\text{-}IA^s$ complex (Fig. 4A) compared to $Y^{78}B$ in the crystal, which does not allow this kind of rotation. The cyclic-Cit peptide appears to have different occupancies of some residues due to is conformational restrictions. Particularly, side chain of H^{88}, which is positioned in between P1 and P2 and side chains V^{87}, A^{96}, Cit^{97} and T^{98} which face towards the exposed region (Fig. 4B). According to our previous work on $H2\text{-}IA^s$,[8, 9] residues H^{88}, F^{89} and K^{91} of the linear MBP peptide point up from the MHC groove and could therefore serve as TCR contacts. The effect of mutations at position 91 have been reported not to cause major disruptions to the structures and to the intermolecular interactions between the peptide and the MHC cleft.[8] Based on crystal structures depicting TCR α and β chains, such as the different in terms of TCR binding HLA-DQ1 - $MBP_{84\text{-}97}$ - Hy.1B11 TCR complex[44], in which the TCR recognition interface is extended towards the MBP residue in position 96 (P^{96}), Cit^{97} of our linear-Cit peptide could potentially affect TCR binding and therefore alter response in comparison to the linear-native peptide.

In the case of the cyclic peptide and in our MD simulations, Cit^{91} firstly interacts with the backbone of the peptide and more specifically backbone atoms of residues 95, 96 and 97 and secondly with Q70B. Therefore, citrulination at position 91 should be more related to the stability of the cyclic peptide itself, or its affinity to $H2\text{-}IA^s$ rather than interacting with TCR. On the other hand, residues in cyclic-Cit peptide pointing towards the T cell recognition site according to our structural model are mainly V^{87}, A^{96}, Cit^{97} and T^{98} resulting to Cit^{97} being totally exposed as a potential TCR contact residue. Cyclization by itself alters the T cell recognition interface of the peptide due to the aforementioned different residues being exposed to make contact with the TCR. Compared to the linear-Cit peptide orientation of, in which citrulline in position 97, is relatively distant to the MHC cleft, in the case of cyclic-Cit, it is well exposed to the TCR interaction interface (Fig. 4B). This totally different topology of the cyclic-Cit peptide could potentially lead to altered TCR recognition and is likely the reason for altered immune response depicted by increased levels of IFN-γ and IL-4. Moreover, conversion of R^{97} to Cit^{97}, may differentiate T cell response through its direct interaction with the receptor.
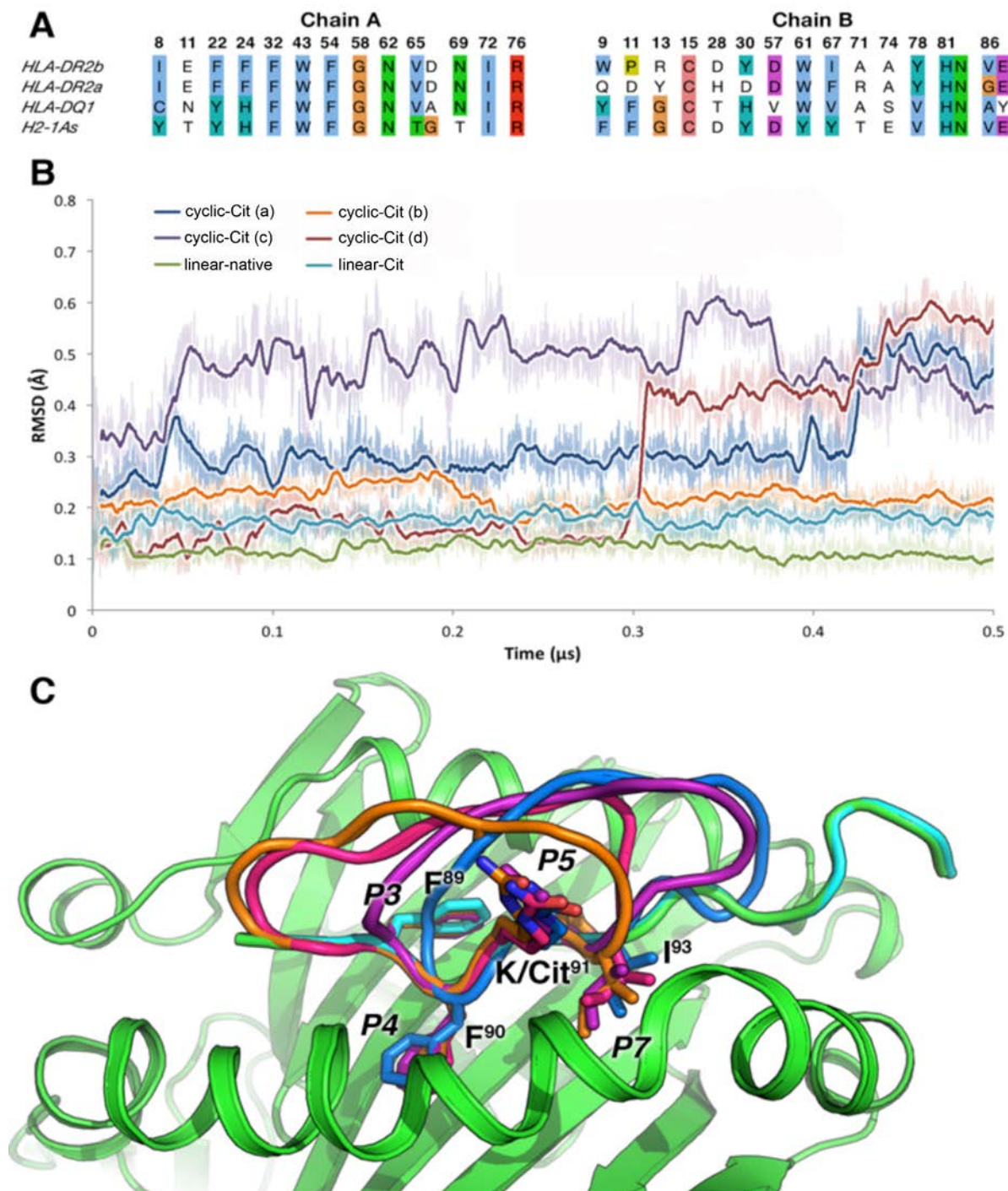
Figure 3. (A) HLA pocket residues in HLA – MBP peptide crystal structures that are involved in forming the cavity for peptide recognition and their corresponding counterparts in H2-IA[s]. Amino acids are highlighted in ClustalX colors. (B) Root mean squared deviations (in transparent colors) of the molecular dynamics simulations of the two linear (linear-native and linear-Cit) P1-P9 occupying residues and cyclic-Cit in their different (a-d) binding orientations. Mean RMSD values refer to peptide backbone atoms and are shown in bold lines. (C) The four different starting docking positions of the cyclic-Cit peptide shown in orange, magenta, red and blue cartoon representation. The linear-native and linear-Cit are shown in cyan and green respectively.
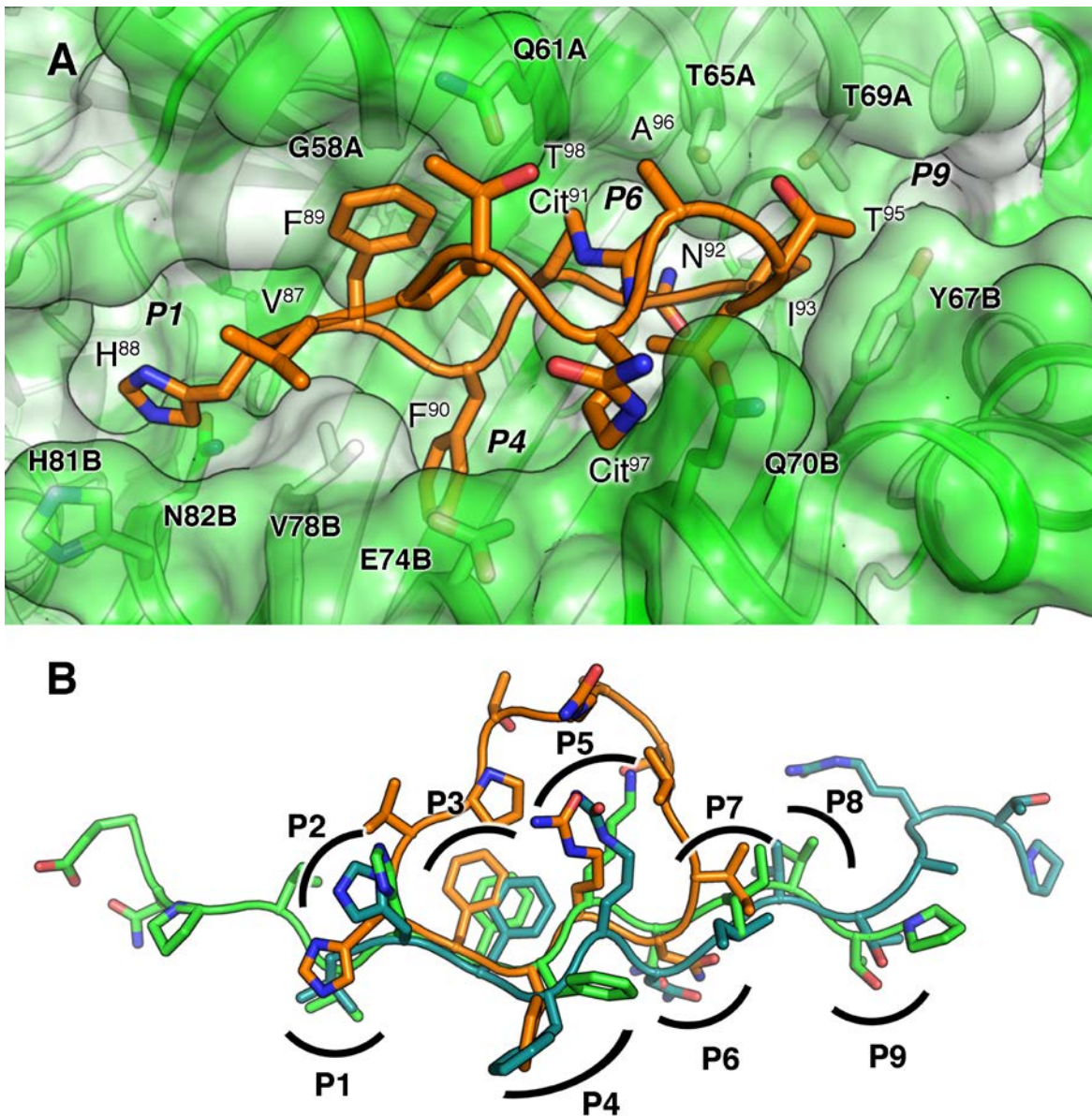
Figure 4. (A) Surface representation of the H2-IA^s complex bound to cyclic-Cit obtained from molecular dynamics simulations. Surface coloring highlights hydrophobicity, i.e. white intensity corresponds to more hydrophobic residues. The cyclic peptide is depicted in orange color sticks and cartoon representation. (B) Superimposition between the representative conformations of simulated linear-Cit (cyan), cyclic-Cit (orange) and linear-native (green) from the HLA-DR2b crystal structure.

3. Conclusion

The immunogenicity of linear-Cit and cyclic-Cit peptides in mice is a first report, which gives insights into the triggers of the disease. Cyclic-Cit peptide conjugated to reduced mannan induced strong IFN-γ and IL-4 cytokine responses and no IL-10. Furthermore, strong T cell proliferative responses were observed. Interestingly, mice immunized with linear-Cit peptide conjugated to reduced mannan did not stimulate T cells in T proliferation assays but

induced weak IL-4 with no IFN-γ and IL-10 responses. These studies demonstrate that cyclic-Cit peptide induces strong T cell responses which secrete IFN-γ and IL-4. From a structural point of view, this may be assumed from an altered TCR interacting interface of the cyclic-Cit compared to the linear-Cit peptide. This finding may open new avenues in drug design of new substances that inhibit PAD enzymes (citrullination) as a therapeutic strategy for the disease. Indeed, small molecule inhibitors of PAD enzymes have been identified using *in silico* screening of commercial libraries which reduce CD3^{+} T cells in mice.[49]

4. Experimental section

4.1. Solid-phase peptide synthesis of cyclic-Cit

The linear-Cit protected peptide (H-Val-His(Trt)-Phe-Phe-**Cit**[91]-Asn(Trt)-Ile-Val-Thr(tBu)-**Ala**[96]-**Cit**[97]-Thr(tBu)-Pro-OH was synthesized on 2-chlorotrityl chloride resin (CTLR-Cl) using the Fmoc/tBu methodology (Scheme 3).[25, 50-52] The Fmoc-protected amino acids were purchased from CBL (Chemical and Biopharmaceutical Laboratories, Patras, Greece). The peptide was synthesized manually on a 0.5 mmol scale, following convergent protocol of solid phase peptide synthesis, up to the final protected analog. The use of the CLTR-Cl under mild conditions (DCM/TFE, 7/3) for cleaving the peptide-resin bond, resulted in the release of high yield and purity of the protected peptide. Yield of fully protected peptide-resins was estimated to be 90 %. Cyclization of linear protected (Cit[91],A[96],Cit[97])MBP$_{87-99}$ (linear-Cit) was accomplished in liquid phase (the concentration of linear protected peptide in DMF was 10^{-5} M) was achieved using *O*-benzotriazol-1-yl-*N,N,N',N'*-tetramethyluronium tetrafluoroborate (TBTU) and 1-hydroxy-7-azabenzotriazole, 2,4,6 collidine in DMF solution, allowing high yield cyclization product (Scheme 3).[7, 22, 53] The monitoring of the cyclization reaction was carried out using the ninhydrin test, and the reaction mixture was resolved by thin-layer chromatography, nbutanol/acetic acid/water (4/1/1) solvent system and analytical RP-HPLC in C4 Nucleosil RP column with 5μm packing material. The protected cyclic analog was then released from side chain protected groups using 90 % trifluoroacetic acid (TFA) in DCM solution containing 5 % Dithiothreitol/Triethylsilane/water/Anisole as scavengers. Semi Preparative RP-HPLC for the purification of linear and cyclic peptide analogs was performed using a Nucleosil RP-18 reverse phase column with a 10 μm pack material 4.6x250 mm. The purity of cyclic peptide was estimated to be 98 % according to the analytical RP-HPLC. The identification of synthesized peptides was achieved by Electron Spray Ionization Mass Spectrometry (ESI-MS) (Figure 5).
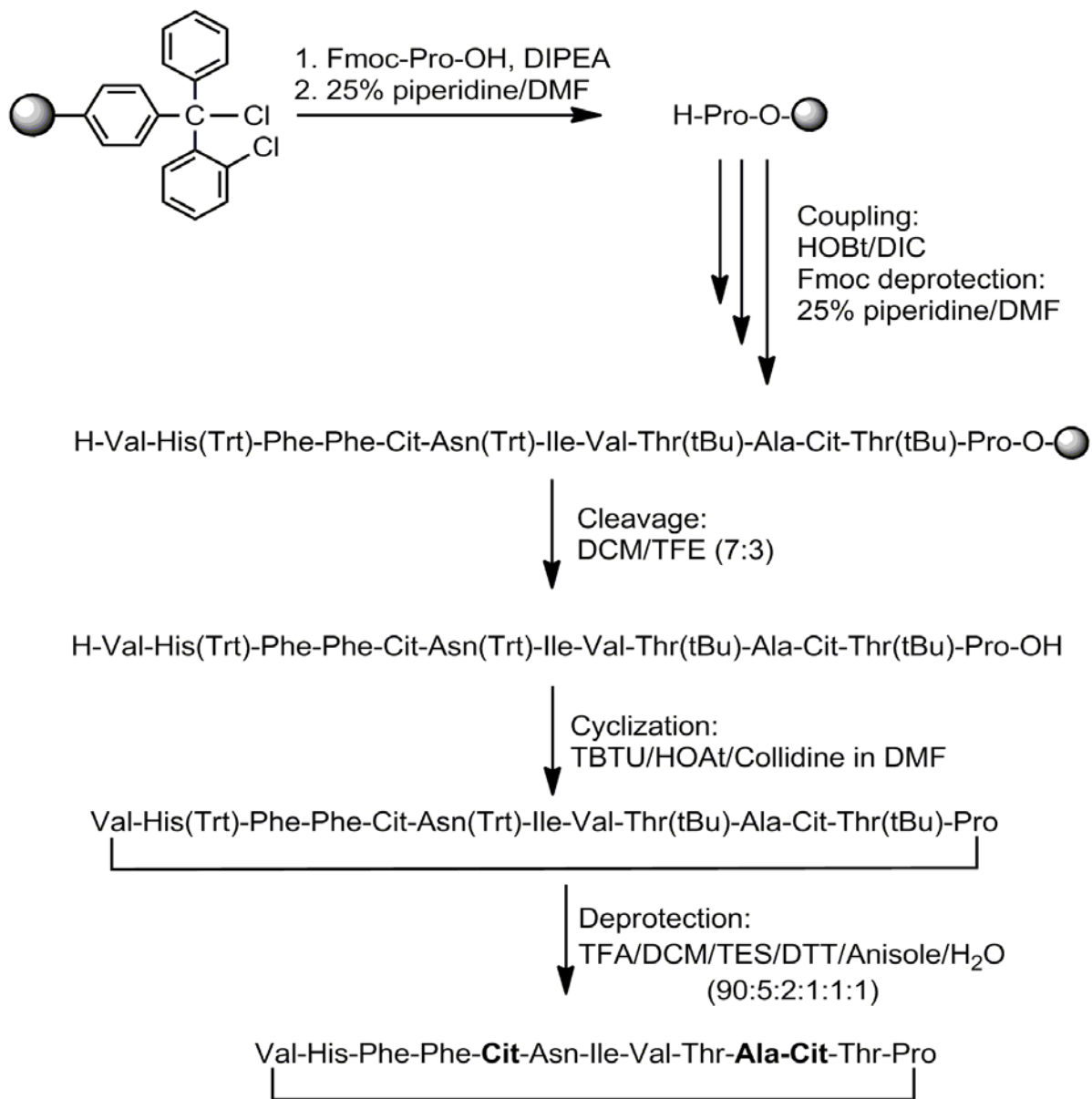
Scheme 3. Synthetic procedure of cyclo(87-99)[Cit^{91},A^{96},Cit^{97}]MBP$_{87-99}$ (cyclic-Cit) peptide
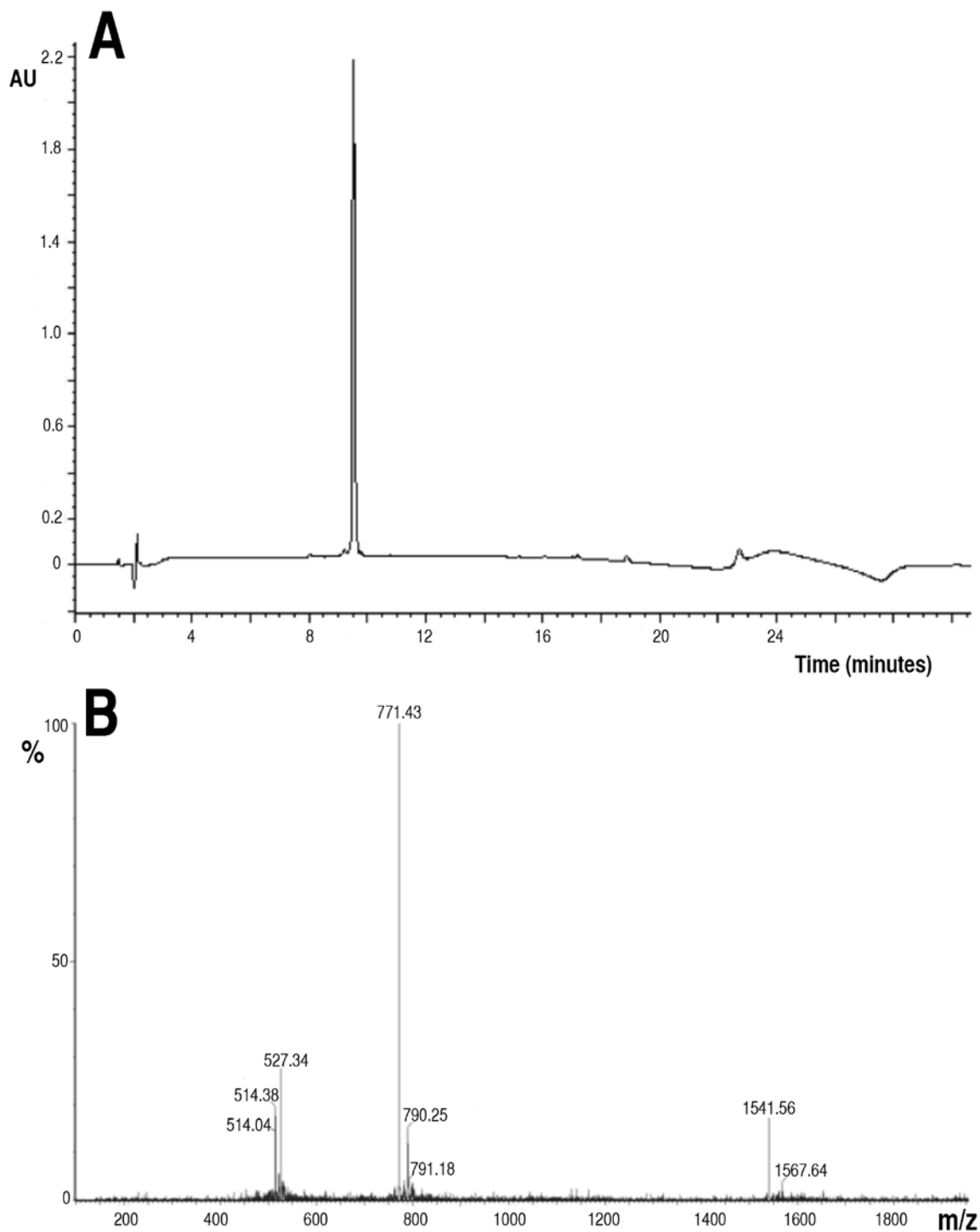
Figure 5. (A) Analytical RP-HPLC of purified (purity 95%) cyclic-Cit analog. Column: Xbridge C18, 150mm×4.6 mm, 3.5µm packing (Part/N= 186003034). RT: 9.49min Conditions: gradient 5% (B)-100% (B), in 30 min, flow rate 1 mL/min. [Eluents (a): solution TFA in H_2O 0.1% (v/v), (b): solution TFA in AcN 0.1% (v/v)]. (B) ESI+MS of cyclic-Cit analog. M+: 1541.56, M +2H+/2: 771.43.27, M +3H+/3: 514.38. [M +2H+/2 +K+: 790.25, M +3H+/3+ K+: 527.34].

4.2. Conjugation of Reduced Mannan to linear-Cit and cyclic-Cit Peptide Analogs

The conjugation between peptide to reduced mannan was achieved following a previously described protocol.[1, 7-10, 52, 54] Briefly, 14 mg mannan (poly-mannose from *Saccharomyces cerevisiae,* Sigma-Aldrich VIC Australia) was dissolved in 1 ml phosphate buffer, pH 6.0, and oxidized with sodium periodate. The oxidized form of mannan was purified using Sephadex G-25 M column pre-equilibrated with bicarbonate buffer pH 9.0. The conjugation of peptide to KLH and then to oxidized mannan was performed in bicarbonate buffer, pH 9.0. The reduced form of mannan was obtained after the addition of sodium borohydride to oxidized mannan-KLH-peptide conjugation.[55-57] Previously we demonstrated that the conjugation efficacy of peptides or proteins to mannan via SDS-PAGE gels, tricine-PAGE gels and capillary electrophoresis to be 100 % conjugated.[58-60]

4.3. Mice and Immunizations

Female 6-8 week old SJL/J mice used in all experiments, were purchased from Walter and Eliza Hall Institute (VIC, Australia) and housed at animal facility of AMREP, Burnet Institute, Australia. SJL/J mice were immunized with 50 μg of each peptide-KLH-reduced mannan, twice on days 0 and 14, intradermally (at the base of the tail). All studies were reviewed and approved by Austin Health and Alfred Health Animal Ethics Committee.

4.4. Immunological assays

4.4.1. ELISpot assay

Spleen cells from immunized SJL/J mice were isolated 14 days after the last immunization and assessed by ELISpot for IFN-γ, IL-4 and IL-10 secretion by T cells as previously described.[1, 7-10, 52, 54] Spots of activity were detected using a colorimetric AP kit (Biorad, Hercules, CA USA) and counted using an AID ELISpot plate reader (Autoimmun Diagnostika GmbH, Germany). Data are presented as mean spot forming units (SFU) per 1.0 x 10^6 cells.

4.4.2. Proliferation Assay

Spleen cells from immunized SJL/J mice were isolated 25-28 days after the second injection and assessed by [^{3}H]-thymidine uptake of cells. 1 x 10^5 spleen cells in 100 μl of culture media were seeded into 96 well U-bottom plates and incubated for 1-5 days at 37 °C in the presence of recall peptide (10 μg/ml), ConA (internal control) or no peptide (negative control). ConA (internal positive control) yielded proliferation of more than 90,000 cpm and was excluded from the figures and no peptide (cells alone) was used as background negative control. [^{3}H]-thymidine uptake was measured using a β-scintillation counter (Top Count Gamma Counter, Packard, USA).

4.5. Homology modeling

The H2-IA^u complex, comprising of the MBP$_{1-11}$ peptide crystal structure (PDB ID: 1k2d; 2.20 Å resolution)[61] was used as a template for the H2-IA^s complex homology model as in previous studies.[8, 9] The primary sequence of the two chains were obtained from the Universal Protein Resource (UNIPROT) database (UNIPROT IDs: P14437.1 and P06345.1 respectively). The homology model was built using MODELLER v9.7[62] and the construction involved the disulfide bonds between C107 - C163 in chain A and C15 – C79 and C117 – C173 in chain B. The overall stereochemical quality of the final model was evaluated by the discrete optimized energy (DOPE)[63] and thorough visual inspection.

4.6. Docking

The linear peptides were docked in the cleft by means of structural alignment according to the MBP peptide bound to HLA-DR2b (PDB ID: 1bx2[64]) crystal structure. In the case of linear-Cit residues in positions 91, 96 and 97 were mutated manually. The cyclic-Cit peptide was docked in four different poses. All of them retained F^{90} and N^{92} in pockets P4 and P6 and were energy minimized using the conjugate gradient algorithm.

4.7. Molecular Dynamics (MD)

All MD simulations were performed using the GROMACS software v4.5.5.[65] Following the structural model, a minimization of the receptor topology was performed in order to remove steric clashes between the residues. The minimized topology was then inserted in a pre-equilibrated box containing water and a 0.15 M concentration of Na and Cl ions. The latest AMBER99SB-ILDN[66] force field was used for all the dynamics simulations along with the TIP3P water model. Force field parameters for l-citrulline were generated using the general Amber force field (GAFF) and HF/6-31G*-derived RESP atomic charges.[67] New, manual amino acid entries were added to the forcefield parameters in order to enable cyclization. Each system consisted of the protein, the peptide, ~15,000 water molecules and ~130 ions in an 8x8x8 nm simulation box. The 6 model systems were energy minimized and subsequently subjected to a 10 ns MD equilibration, with positional restraints on protein coordinates. These restraints were released, and 500 ns MD trajectories were produced in constant temperature of 300 K using separate v-rescale thermostats for the protein, the peptide and solvent molecules. A time step of 2 fs was used and all bonds were constrained using the LINCS algorithm. Lennard-Jones interactions were computed using a cut-off of 10 Å, and the electrostatic interactions were treated using PME with the same real-space cut-off.

Acknowledgements

References

1.   Katsara, M.; Matsoukas, J.; Deraos, G.; Apostolopoulos, V. Towards immunotherapeutic drugs and vaccines against multiple sclerosis. *Acta Biochim Biophys Sin (Shanghai)* **2008,** 40, 636-42.

2.   Mantzourani, E. D.; Mavromoustakos, T. M.; Platts, J. A.; Matsoukas, J. M.; Tselios, T. V. Structural requirements for binding of myelin basic protein (MBP) peptides to MHC II: effects on immune regulation. *Curr Med Chem* **2005,** 12, 1521-35.

3.   Babaloo, Z.; Aliparasti, M. R.; Babaiea, F.; Almasi, S.; Baradaran, B.; Farhoudi, M. The role of Th17 cells in patients with relapsing-remitting multiple sclerosis: interleukin-17A and interleukin-17F serum levels. *Immunol Lett* **2015,** 164, 76-80.

4.   Degano, M.; Garcia, K. C.; Apostolopoulos, V.; Rudolph, M. G.; Teyton, L.; Wilson, I. A. A functional hot spot for antigen recognition in a superagonist TCR/MHC complex. *Immunity* **2000,** 12, 251-61.

5.   Evavold, B. D.; Sloan-Lancaster, J.; Allen, P. M. Tickling the TCR: selective T-cell functions stimulated by altered peptide ligands. *Immunol Today* **1993,** 14, 602-9.

6.   Hedegaard, C. J.; Krakauer, M.; Bendtzen, K.; Lund, H.; Sellebjerg, F.; Nielsen, C. H. T helper cell type 1 (Th1), Th2 and Th17 responses to myelin basic protein and disease activity in multiple sclerosis. *Immunology* **2008**.

7.   Katsara, M.; Deraos, G.; Tselios, T.; Matsoukas, J.; Apostolopoulos, V. Design of novel cyclic altered peptide ligands of myelin basic protein MBP83-99 that modulate immune responses in SJL/J mice. *J Med Chem* **2008,** 51, 3971-8.

8.   Katsara, M.; Yuriev, E.; Ramsland, P. A.; Deraos, G.; Tselios, T.; Matsoukas, J.; Apostolopoulos, V. A double mutation of MBP(83-99) peptide induces IL-4 responses and antagonizes IFN-gamma responses. *J Neuroimmunol* **2008,** 200, 77-89.

9.   Katsara, M.; Yuriev, E.; Ramsland, P. A.; Deraos, G.; Tselios, T.; Matsoukas, J.; Apostolopoulos, V. Mannosylation of mutated MBP83-99 peptides diverts immune responses from Th1 to Th2. *Mol Immunol* **2008,** 45, 3661-70.

10.   Mouzaki, A.; Tselios, T.; Papathanassopoulos, P.; Matsoukas, I.; Chatzantoni, K. Immunotherapy for multiple sclerosis: basic insights for new clinical strategies. *Curr Neurovasc Res* **2004,** 1, 325-40.

11.   Kalergis, A. M.; Nathenson, S. G. Altered peptide ligand-mediated TCR antagonism can be modulated by a change in a single amino acid residue within the CDR3 beta of an MHC class I-restricted TCR. *J Immunol* **2000,** 165, 280-5.

12.   Thomson, C. T.; Kalergis, A. M.; Sacchettini, J. C.; Nathenson, S. G. A structural difference limited to one residue of the antigenic peptide can profoundly alter the biological outcome of the TCR-peptide/MHC class I interaction. *J Immunol* **2001,** 166, 3994-7.

13.   Chen, J.; Im, W.; Brooks, C. L. Balancing Solvation and Intramolecular Interactions: Toward a Consistent Generalized Born Force Field. *J. Am. Chem. Soc* **2006,** 128, 3728-3736.

14. Bielekova, B.; Goodwin, B.; Richert, N.; Cortese, I.; Kondo, T.; Afshar, G.; Gran, B.; Eaton, J.; Antel, J.; Frank, J. A.; McFarland, H. F.; Martin, R. Encephalitogenic potential of the myelin basic protein peptide (amino acids 83-99) in multiple sclerosis: results of a phase II clinical trial with an altered peptide ligand. *Nat Med* **2000,** 6, 1167-75.

15. Crowe, P. D.; Qin, Y.; Conlon, P. J.; Antel, J. P. NBI-5788, an altered MBP83-99 peptide, induces a T-helper 2-like immune response in multiple sclerosis patients. *Ann Neurol* **2000,** 48, 758-65.

16. Kappos, L.; Comi, G.; Panitch, H.; Oger, J.; Antel, J.; Conlon, P.; Steinman, L. Induction of a non-encephalitogenic type 2 T helper-cell autoimmune response in multiple sclerosis after administration of an altered peptide ligand in a placebo-controlled, randomized phase II trial. The Altered Peptide Ligand in Relapsing MS Study Group. *Nat Med* **2000,** 6, 1176-82.

17. Kim, H. J.; Antel, J. P.; Duquette, P.; Alleva, D. G.; Conlon, P. J.; Bar-Or, A. Persistence of immune responses to altered and native myelin antigens in patients with multiple sclerosis treated with altered peptide ligand. *Clin Immunol* **2002,** 104, 105-14.

18. Mantzourani, E. D.; Platts, J. A.; Brancale, A.; Mavromoustakos, T. M.; Tselios, T. V. Molecular dynamics at the receptor level of immunodominant myelin basic protein epitope 87-99 implicated in multiple sclerosis and its antagonists altered peptide ligands: triggering of immune response. *J Mol Graph Model* **2007,** 26, 471-81.

19. Mantzourani, E. D.; Tselios, T. V.; Grdadolnik, S. G.; Brancale, A.; Platts, J. A.; Matsoukas, J. M.; Mavromoustakos, T. M. A putative bioactive conformation for the altered peptide ligand of myelin basic protein and inhibitor of experimental autoimmune encephalomyelitis [Arg91, Ala96] MBP87-99. *J Mol Graph Model* **2006,** 25, 17-29.

20. Mantzourani, E. D.; Tselios, T. V.; Grdadolnik, S. G.; Platts, J. A.; Brancale, A.; Deraos, G. N.; Matsoukas, J. M.; Mavromoustakos, T. M. Comparison of proposed putative active conformations of myelin basic protein epitope 87-99 linear altered peptide ligands by spectroscopic and modelling studies: the role of positions 91 and 96 in T-cell receptor activation. *J Med Chem* **2006,** 49, 6683-91.

21. Spyranti, Z.; Dalkas, G. A.; Spyroulias, G. A.; Mantzourani, E. D.; Mavromoustakos, T.; Friligou, I.; Matsoukas, J. M.; Tselios, T. V. Putative bioactive conformations of amide linked cyclic myelin basic protein peptide analogues associated with experimental autoimmune encephalomyelitis. *J Med Chem* **2007,** 50, 6039-47.

22. Tselios, T.; Apostolopoulos, V.; Daliani, I.; Deraos, S.; Grdadolnik, S.; Mavromoustakos, T.; Melachrinou, M.; Thymianou, S.; Probert, L.; Mouzaki, A.; Matsoukas, J. Antagonistic effects of human cyclic MBP(87-99) altered peptide ligands in experimental allergic encephalomyelitis and human T-cell proliferation. *J Med Chem* **2002,** 45, 275-83.

23. Tselios, T.; Probert, L.; Daliani, I.; Matsoukas, E.; Troganis, A.; Gerothanassis, I. P.; Mavromoustakos, T.; Moore, G. J.; Matsoukas, J. M. Design and synthesis of a potent cyclic analogue of the myelin basic protein epitope MBP72-85: importance of the Ala81 carboxyl group and of a cyclic conformation for induction of experimental allergic encephalomyelitis. *J Med Chem* **1999,** 42, 1170-7.

24. Tselios, T.; Daliani, I.; Probert, L.; Deraos, S.; Matsoukas, E.; Roy, S.; Pires, J.; Moore, G.; Matsoukas, J. Treatment of experimental allergic encephalomyelitis (EAE) induced by guinea pig myelin basic protein epitope 72-85 with a human MBP(87-99) analogue and effects of cyclic peptides. *Bioorg Med Chem* **2000,** 8, 1903-9.

25. Matsoukas, J.; Apostolopoulos, V.; Kalbacher, H.; Papini, A. M.; Tselios, T.; Chatzantoni, K.; Biagioli, T.; Lolli, F.; Deraos, S.; Papathanassopoulos, P.; Troganis, A.; Mantzourani, E.; Mavromoustakos, T.; Mouzaki, A. Design and synthesis of a novel potent myelin basic protein epitope 87-99 cyclic analogue: enhanced stability and biological properties of mimics render them a potentially new class of immunomodulators. *J Med Chem* **2005,** 48, 1470-80.

26. Baka, Z.; Gyorgy, B.; Geher, P.; Buzas, E. I.; Falus, A.; Nagy, G. Citrullination under physiological and pathological conditions. *Joint Bone Spine* **2012,** 79, 431-6.

27. Horibata, S.; Coonrod, S. A.; Cherrington, B. D. Role for peptidylarginine deiminase enzymes in disease and female reproduction. *J Reprod Dev* **2012,** 58, 274-82.

28. Deraos, G.; Chatzantoni, K.; Matsoukas, M. T.; Tselios, T.; Deraos, S.; Katsara, M.; Papathanasopoulos, P.; Vynios, D.; Apostolopoulos, V.; Mouzaki, A.; Matsoukas, J. Citrullination of linear and cyclic altered peptide ligands from myelin basic protein (MBP(87-99)) epitope elicits a Th1 polarized response by T cells isolated from multiple sclerosis patients: implications in triggering disease. *J Med Chem* **2008,** 51, 7834-42.

29. Pritzker, L. B.; Joshi, S.; Gowan, J. J.; Harauz, G.; Moscarello, M. A. Deimination of myelin basic protein. 1. Effect of deimination of arginyl residues of myelin basic protein on its structure and susceptibility to digestion by cathepsin D. *Biochemistry* **2000,** 39, 5374-81.

30. Pritzker, L. B.; Joshi, S.; Harauz, G.; Moscarello, M. A. Deimination of myelin basic protein. 2. Effect of methylation of MBP on its deimination by peptidylarginine deiminase. *Biochemistry* **2000,** 39, 5382-8.

31. Bradford, C. M.; Ramos, I.; Cross, A. K.; Haddock, G.; McQuaid, S.; Nicholas, A. P.; Woodroofe, M. N. Localisation of citrullinated proteins in normal appearing white matter and lesions in the central nervous system in multiple sclerosis. *J Neuroimmunol* **2014,** 273, 85-95.

32. Martin, R.; Whitaker, J. N.; Rhame, L.; Goodin, R. R.; McFarland, H. F. Citrulline-containing myelin basic protein is recognized by T-cell lines derived from multiple sclerosis patients and healthy individuals. *Neurology* **1994,** 44, 123-9.

33. Whitaker, J. N.; Kirk, K. A.; Herman, P. K.; Zhou, S. R.; Goodin, R. R.; Moscarello, M. A.; Wood, D. D. An immunochemical comparison of human myelin basic protein and its modified, citrullinated form, C8. *J Neuroimmunol* **1992,** 36, 135-46.

34. Sommer, N.; Martin, R.; McFarland, H. F.; Quigley, L.; Cannella, B.; Raine, C. S.; Scott, D. E.; Loschmann, P. A.; Racke, M. K. Therapeutic potential of phosphodiesterase type 4 inhibition in chronic autoimmune demyelinating disease. *J Neuroimmunol* **1997,** 79, 54-61.

35. Kalbus, M.; Fleckenstein, B. T.; Offenhausser, M.; Bluggel, M.; Melms, A.; Meyer, H. E.; Rammensee, H. G.; Martin, R.; Jung, G.; Sommer, N. Ligand motif of the autoimmune disease-associated mouse MHC class II molecule H2-A(s). *Eur J Immunol* **2001,** 31, 551-62.

36. Yang, L.; Tan, D.; Piao, H. Myelin Basic Protein Citrullination in Multiple Sclerosis: A Potential Therapeutic Target for the Pathology. *Neurochem Res* **2016**.

37. Moscarello, M. A.; Mastronardi, F. G.; Wood, D. D. The role of citrullinated proteins suggests a novel mechanism in the pathogenesis of multiple sclerosis. *Neurochem Res* **2007,** 32, 251-6.

38. Tranquill, L. R.; Cao, L.; Ling, N. C.; Kalbacher, H.; Martin, R. M.; Whitaker, J. N. Enhanced T cell responsiveness to citrulline-containing myelin basic protein in multiple sclerosis patients. *Mult Scler* **2000,** 6, 220-5.

39. Apostolopoulos, V.; Barnes, N.; Pietersz, G. A.; McKenzie, I. F. Ex vivo targeting of the macrophage mannose receptor generates anti-tumor CTL responses. *Vaccine* **2000,** 18, 3174-84.

40. Apostolopoulos, V.; McKenzie, I. F. Role of the mannose receptor in the immune response. *Curr Mol Med* **2001,** 1, 469-74.

41. Katsara, M.; Yuriev, E.; Ramsland, P. A.; Deraos, G.; Lourbopoulos, A.; Grigoriadis, N.; Matsoukas, J.; Apostolopoulos, V. Altered peptide ligands of myelin basic protein (MBP$_{87-99}$) conjugated to reduced mannan modulate immune responses in mice. *Immunology* **2009,** 128, 521-33

42. Hahn, M.; Nicholson, M. J.; Pyrdol, J.; Wucherpfennig, K. W. Unconventional topology of self peptide–major histocompatibility complex binding by a human autoimmune T cell receptor. *Nature immunology* **2005,** 6, 490-496.

43.   Smith, K. J.; Pyrdol, J.; Gauthier, L.; Wiley, D. C.; Wucherpfennig, K. W. Crystal structure of HLA-DR2 (DRA* 0101, DRB1* 1501) complexed with a peptide from human myelin basic protein. *The Journal of experimental medicine* **1998,** 188, 1511-1520.

44.   Sethi, D. K.; Schubert, D. A.; Anders, A.-K.; Heroux, A.; Bonsor, D. A.; Thomas, C. P.; Sundberg, E. J.; Pyrdol, J.; Wucherpfennig, K. W. A highly tilted binding mode by a self-reactive T cell receptor results in altered engagement of peptide and MHC. *The Journal of experimental medicine* **2011,** 208, 91-102.

45.   Li, Y.; Li, H.; Martin, R.; Mariuzza, R. A. Structural basis for the binding of an immunodominant peptide from myelin basic protein in different registers by two HLA-DR2 proteins. *Journal of molecular biology* **2000,** 304, 177-188.

46.   Li, Y.; Li, H.; Dimasi, N.; McCormick, J. K.; Martin, R.; Schuck, P.; Schlievert, P. M.; Mariuzza, R. A. Crystal structure of a superantigen bound to the high-affinity, zinc-dependent site on MHC class II. *Immunity* **2001,** 14, 93-104.

47.   Li, Y.; Huang, Y.; Lue, J.; Quandt, J. A.; Martin, R.; Mariuzza, R. A. Structure of a human autoimmune TCR bound to a myelin basic protein self-peptide and a multiple sclerosis-associated MHC class II molecule. *The EMBO journal* **2005,** 24, 2968-2979.

48.   Hahn, M.; Nicholson, M. J.; Pyrdol, J.; Wucherpfennig, K. W. Unconventional topology of self peptide-major histocompatibility complex binding by a human autoimmune T cell receptor. *Nat Immunol* **2005,** 6, 490-6.

49.   Wei, L.; Wasilewski, E.; Chakka, S. K.; Bello, A. M.; Moscarello, M. A.; Kotra, L. P. Novel inhibitors of protein arginine deiminase with potential activity in multiple sclerosis animal model. *J Med Chem* **2013,** 56, 1715-22.

50.   Friligou, I.; Rizzolo, F.; Nuti, F.; Tselios, T.; Evangelidou, M.; Emmanouil, M.; Karamita, M.; Matsoukas, J.; Chelli, M.; Rovero, P.; Papini, A. M. Divergent and convergent synthesis of polymannosylated dibranched antigenic peptide of the immunodominant epitope MBP(83-99). *Bioorg Med Chem* **2013,** 21, 6718-25.

51.   Ieronymaki, M.; Androutsou, M. E.; Pantelia, A.; Friligou, I.; Crisp, M.; High, K.; Penkman, K.; Gatos, D.; Tselios, T. Use of the 2-chlorotrityl chloride resin for microwave-assisted solid phase peptide synthesis. *Biopolymers* **2015,** 104, 506-14.

52.   Katsara, M.; Deraos, G.; Tselios, T.; Matsoukas, M. T.; Friligou, I.; Matsoukas, J.; Apostolopoulos, V. Design and synthesis of a cyclic double mutant peptide (cyclo(87-99)[A91,A96]MBP87-99) induces altered responses in mice after conjugation to mannan: implications in the immunotherapy of multiple sclerosis. *J Med Chem* **2009,** 52, 214-8.

53.   Ehrlich, A.; Heyne, H. U.; Winter, R.; Beyermann, M.; Haber, H.; Carpino, L. A.; Bienert, M. Cyclization of all-L-Pentapeptides by Means of 1-Hydroxy-7-azabenzotriazole-Derived Uronium and Phosphonium Reagents. *J Org Chem* **1996,** 61, 8831-8838.

54.   Katsara, M.; Tselios, T.; Deraos, S.; Deraos, G.; Matsoukas, M. T.; Lazoura, E.; Matsoukas, J.; Apostolopoulos, V. Round and round we go: cyclic peptides in disease. *Curr Med Chem* **2006,** 13, 2221-32.

55.   Apostolopoulos, V.; Pietersz, G. A.; Gordon, S.; Martinez-Pomares, L.; McKenzie, I. F. Aldehyde-mannan antigen complexes target the MHC class I antigen-presentation pathway. *Eur J Immunol* **2000,** 30, 1714-23.

56.   Apostolopoulos, V.; Pietersz, G. A.; Loveland, B. E.; Sandrin, M. S.; McKenzie, I. F. Oxidative/reductive conjugation of mannan to antigen selects for T1 or T2 immune responses. *Proc Natl Acad Sci U S A* **1995,** 92, 10128-32.

57.   Apostolopoulos, V.; Pietersz, G. A.; Xing, P. X.; Lees, C. J.; Michael, M.; Bishop, J.; McKenzie, I. F. The immunogenicity of MUC1 peptides and fusion protein. *Cancer Lett* **1995,** 90, 21-6.

58.   Apostolopoulos, V.; Pietersz, G. A.; McKenzie, I. F. Cell-mediated immune responses to MUC1 fusion protein coupled to mannan. *Vaccine* **1996,** 14, 930-938.

59.   Tselios, T.; Lamari, F. N.; Karathanasopoulou, I.; Katsara, M.; Apostolopoulos, V.; Pietersz, G. A.; Matsoukas, J.; Karamanos, N. K. Synthesis and study of the electrophoretic behavior of

mannan conjugates with cyclic peptide analogue of myelin basic protein using lysine-glycine linker. *Analytical Biochemistry* **2005,** 347, 121-128.

60. Tapeinou, A.; Androutsou, M-E.; Kyrtata, K.; **Apostolopoulos, V**.; Matsoukas, J.; Tselios, T. Evaluation of the conjugation of MOG$_{35-55}$ peptide epitope to mannan by tricine SDS-PAGE. *Analytical Biochemistry* **2015,** 485, 43-45.

61. He, X.-l.; Radu, C.; Sidney, J.; Sette, A.; Ward, E. S.; Garcia, K. C. Structural snapshot of aberrant antigen presentation linked to autoimmunity: the immunodominant epitope of MBP complexed with I-Au. *Immunity* **2002,** 17, 83-94.

62. Webb, B.; Sali, A. Comparative protein structure modeling using Modeller. *Current protocols in bioinformatics* **2014,** 5.6. 1-5.6. 32.

63. Shen, M. y.; Sali, A. Statistical potential for assessment and prediction of protein structures. *Protein science* **2006,** 15, 2507-2524.

64. Jones, E. Y.; Fugger, L.; Strominger, J. L.; Siebold, C. MHC class II proteins and disease: a structural perspective. *Nature Reviews Immunology* **2006,** 6, 271-282.

65. Pronk, S.; Páll, S.; Schulz, R.; Larsson, P.; Bjelkmar, P.; Apostolov, R.; Shirts, M. R.; Smith, J. C.; Kasson, P. M.; van der Spoel, D. GROMACS 4.5: a high-throughput and highly parallel open source molecular simulation toolkit. *Bioinformatics* **2013,** 29, 845-854.

67. Lindorff-Larsen, K.; Piana, S.; Palmo, K.; Maragakis, P.; Klepeis, J. L.; Dror, R. O.; Shaw, D. E. Improved side-chain torsion potentials for the Amber ff99SB protein force field. *Proteins: Structure, Function, and Bioinformatics* **2010,** 78, 1950-1958.

68. Bayly, C. I.; Cieplak, P.; Cornell, W.; Kollman, P. A. A well-behaved electrostatic potential based method using charge restraints for deriving atomic charges: the RESP model. *The Journal of Physical Chemistry* **1993,** 97, 10269-10280.